

Multiband Vector Lattice Solitons

Oren Cohen,¹ Tal Schwartz,¹ Jason W. Fleischer,^{1,2} Mordechai Segev,¹ and Demetrios N. Christodoulides²

¹*Department of Physics and Solid State Institute, Technion, Haifa 32000, Israel*

²*School of Optics/CREOL, University of Central Florida, Florida 32816-2700, USA*

(Received 6 February 2003; published 10 September 2003)

We predict multiband vector solitons in nonlinear periodic systems, using photonic lattices as a prime example. The solitons consist of two optical fields arising from different bands of the transmission spectrum, which involve both bound state and radiation mode components.

DOI: 10.1103/PhysRevLett.91.113901

PACS numbers: 42.65.Tg, 42.65.Wi

Solitons in nonlinear periodic systems (lattices) play a fundamental role in many branches of science, such as biology [1], nonlinear optics [2], solid state physics [3], and Bose-Einstein condensates (BEC) [4]. In these systems, the dynamics are determined by a competition between transport (dispersion/diffraction) effects and nonlinearity. In optics, the paradigm example is propagation in nonlinear waveguide arrays [2,5–13]. The linear eigenmodes of such periodic structures are Floquet-Bloch (FB) waves, with their transmission spectra divided into bands, separated by gaps in which propagating modes do not exist [14]. In general, bands originate from either guided modes, which are bound within channels and decay outside, or radiation modes, which oscillate in the space between channels. If the structure is made of a chain of potential wells, each having a single bound state, then the first band arises from the guided modes, whereas all higher bands stem from radiation modes. The FB waves extend over the entire array, so that an excitation of a localized wave packet (a superposition of FB waves) leads to broadening (diffraction) during propagation. In contrast to homogeneous media, diffraction in periodic systems can be normal or anomalous depending on whether the corresponding Bloch wave vector is near the center or the edge of the Brillouin zone, respectively, for the odd bands, and vice versa for the even bands [15]. When the periodic system is nonlinear (e.g., a nonlinear photonic lattice), the wave can induce (via self-focusing/defocusing) a defect into the periodic potential and consequently localize FB waves to its vicinity, driving their propagation constants (“eigenenergies”) into the gaps. Positive defects (deeper potential or increased refractive index) attract normally diffracting FB waves, whereas negative defects attract anomalously diffracting waves. When a localized wave packet that induces a defect is also an eigenmode of the full potential (lattice plus induced defect), the propagation of the wave packet is stationary; i.e., it is a lattice soliton. A standard approach to study lattice solitons is via the discrete nonlinear Schrödinger equation (DNLS) [2], which treats the array as a chain of nonlinear sites coupled linearly with their nearest neighbors. In this context, scalar (both in the normal [2] and the anomalous [8] diffraction regimes) as well as vector [10]

solitons have been analyzed. However, the DNLS model can describe bands arising from bound states only. On the other hand, lattice solitons resulting from bands involving radiation modes necessitate a continuous model as was developed for grating solitons in fibers [16], and for nonlinear photonic lattices [7,13]. Higher band solitons have been recently observed in waveguide arrays [12].

Here, we present the prediction of multiband vector solitons in nonlinear periodic systems, with an emphasis on photonic lattices. The solitons consist of two fields arising from different bands of the transmission spectrum, which involves both bound-state and radiation mode components. We find multiband bright vector lattice solitons for both self-focusing and defocusing nonlinearities, verify their stability, and discuss their relevance to other systems in nature.

Vector solitons, which have been studied in homogeneous media [17], are solitons consisting of multiple components. They form when their constituents jointly induce a potential and properly populate its bound states [18]. Typically, the interference terms between different modes do not contribute to the induced index change and the system is governed by a Manakov-like model [19–21]. The simplest case is when the components populate the fundamental bound state of the induced potential [19–22]. More interesting are vector solitons whose components belong to different modes of their jointly induced potential [23,24], as observed with optical spatial solitons [25]. For nonlinear periodic systems, however, only first-band vector solitons have been analyzed [10] and observed [11].

While the concept of multiband vector lattice solitons is general, for concreteness we demonstrate their properties in a nonlinear waveguide array. Consider two fields, with envelopes Ψ_1 and Ψ_2 , copropagating along the array (z direction). The linear refractive index is $n = n_0 + \Delta n_0 f(x)$, where n_0 is the index at the barriers, f represents the normalized periodic function describing the structure of the photonic lattice ($0 \leq f \leq 1$), and Δn_0 is its amplitude. We assume a Kerr-like nonlinearity of $\Delta n(I) = n_2 I$, n_2 being the Kerr coefficient and $I = |\Psi_1|^2 + |\Psi_2|^2$. Assuming terms like $\Psi_1 \Psi_2^*$ do not contribute to Δn [18–25], $\Delta n = (\Delta n_0 + n_2 I) \ll n_0$, the

paraxial evolution of $\Psi_{1,2}$ is given by

$$\left\{ i \frac{\partial}{\partial z} + \frac{1}{2k_0} \frac{\partial^2}{\partial x^2} + \frac{k_0}{n_0} [\Delta n_0 f(x) + n_2 I] \right\} \Psi_j = 0, \quad (1)$$

where $k_0 = \omega n_0 / c$, ω is the frequency, c is the vacuum speed of light, and $j = 1, 2$. By introducing $\zeta = \Delta n_0 k_0 z / n_0$, $\xi = \sqrt{2k_0^2 \Delta n_0 / n_0} x$, and $\Phi_j = \Psi_j \sqrt{|n_2| / \Delta n_0}$ Eqs. (1) are transformed into the dimensionless equations

$$\left\{ i \frac{\partial}{\partial \zeta} + \frac{\partial^2}{\partial \xi^2} + f(\xi) + \sigma (|\Phi_1|^2 + |\Phi_2|^2) \right\} \Phi_j = 0, \quad (2)$$

where $\sigma = 1$ (-1) denotes a self-focusing (defocusing) nonlinearity. We seek stationary solutions of Eqs. (2) of the form $\Phi_{1,2} = I_{1,2} u_{1,2}(\xi) \exp(i\beta_{1,2}\zeta)$, where $I_{1,2}$ are the nondimensional peak intensity of each field, $\beta_{1,2}$ are real propagation constants, and $u_{1,2}(\xi)$ are real normalized (to $\sqrt{I_{1,2}}$) functions, which satisfy

$$u''_{1,2} + [f + \sigma(I_1 u_1^2 + I_2 u_2^2)] u_{1,2} = \beta_{1,2} u_{1,2}. \quad (3)$$

Here, the term in the square brackets represents the total potential consisting of the linear (periodic) part $f(\xi)$ and the nonlinear part jointly induced by the waves $u_{1,2}(\xi)$ themselves. When both $I_{1,2}$ are zero, Eqs. (3) are linear, and each eigenmode is a symmetric superposition of two FB waves of the same band with opposite Bloch wave number k_x , so that the transverse momentum of the eigenmode is zero. This results from our choice of seeking real $u_{1,2}(\xi)$. Each mode is characterized by a band index and a Bloch wave number k_x . In the linear case, the modes $u_i(\xi)$ are delocalized. However, when one of the coefficients, say I_1 , is nonzero, then $u_1(\xi)$ induces a defect in the periodic potential $f(\xi)$, which localizes some of the modes. A solution that is a localized mode of its own total potential [linear $f(\xi)$ plus self-induced $I_1 u_1^2$] is a scalar lattice soliton. When both $I_{1,2}$ are nonzero, the solution is a vector (two-component) lattice soliton, which can be degenerate [if $u_1(\xi) = u_2(\xi)$; ‘‘Manakov-like lattice solitons’’] or nondegenerate (multimode) soliton. Multimode lattice solitons can have components (u_1 and u_2) arising from the same band [10,11] or from two different bands. Here we are interested in multiband vector solitons: localized solutions of Eqs. (3) for which $u_1(\xi)$ and $u_2(\xi)$ arise from different bands and reside in different gaps. As an example, consider $u_1(\xi)$ from the first band and $u_2(\xi)$ from the second band, so that the vector soliton is composed of one guided mode and one radiation mode. To identify these solitons [given the periodic potential $f(\xi)$] we seek self-trapped real eigensolutions of Eqs. (3), $u_1(\xi)$ and $u_2(\xi)$, with Bloch wave numbers $k_x^{(1),(2)}$ and peak intensities $I_{1,2}$. The solutions are found by solving Eqs. (3) self-consistently, in the fashion previously used to find multimode solitons in homogeneous media [24].

As a specific example, consider an array function $f(\xi) = \sum_j a(\xi - jD)$, j being an integer, with periodicity $D = 5$, and the index profile of a single waveguide given

by $a(\xi) = \exp[-(\xi/\xi_0)^8]$. We set $\xi_0 = 1.65$ so that the second mode of an isolated single waveguide $a(\xi)$ is slightly above the cutoff (i.e., the waveguide has only one bound state). The profile of such an isolated waveguide $a(\xi)$ along with the shape of its (linear) guided mode are shown in Fig. 1(a). The transverse profile of FB waves of the first and second bands with $k_x = 0$ and $k_x = \pi/D$ are shown in Figs. 1(b)–1(e). The second band FB waves do not decay in the barriers, indicating that they arise from radiation modes. All components of the vector lattice solitons that follow originate from the FB modes shown in Fig. 1.

Figure 2 shows an example of bright vector solitons in a focusing nonlinearity, $\sigma = 1$, with $I_1 = 0.06$ and $I_2 = 0.09$. The first component [Fig. 2(a)] is a localized mode arising from the first band with $k_x^{(1)} = 0$. The second component [Fig. 2(b)] is also a localized mode, yet it arises from the second band with $k_x^{(2)} = \pi/D$. Also shown in Figs. 2(a) and 2(b) is the refractive index: the fixed periodic lattice and the induced index change (forming a positive defect). Figure 2(c) shows the dispersion relation $\beta(k_x)$ of the first three bands of the linear array, with the propagation constants of the two soliton components marked by dots. [In the curve $\beta(k_x)$, all the propagation constants in the second band lay below $\beta = 0$, indicating that the modes of the second band are radiative.] To verify that the solution obtained through self-consistency is indeed a *stable* vector lattice soliton, we simulate its propagation with initial perturbations of white noise. The stationary propagation of the first and second components is shown in Figs. 2(f) and 2(g), respectively. Figures 2(d) and 2(e) show the intensities of the first and second components, at the input (top) and output (bottom). The output intensities are superimposed on the unperturbed profiles obtained through self-consistency (dotted line). The output intensities of both components are almost indistinguishable from those of the ideal vector lattice soliton. Figures 2(h) and 2(i) show the linear propagation of u_1 and u_2 when the nonlinearity is zero. Figure 2(j) shows the propagation of u_1 when the nonlinearity is ‘‘on’’ and u_2 is absent, demonstrating that the first component does not self-trap alone. Similarly, Fig. 2(k) shows

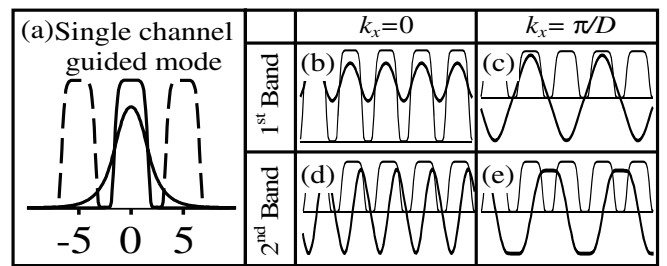


FIG. 1. Confined mode of a single waveguide and its evanescent coupling to the adjacent waveguides (a). Structure of FB waves in the first band at the center (b) and edge (c) of the first Brillouin zone, and also of FB waves in the second band, at the center (d) and the edge (e).

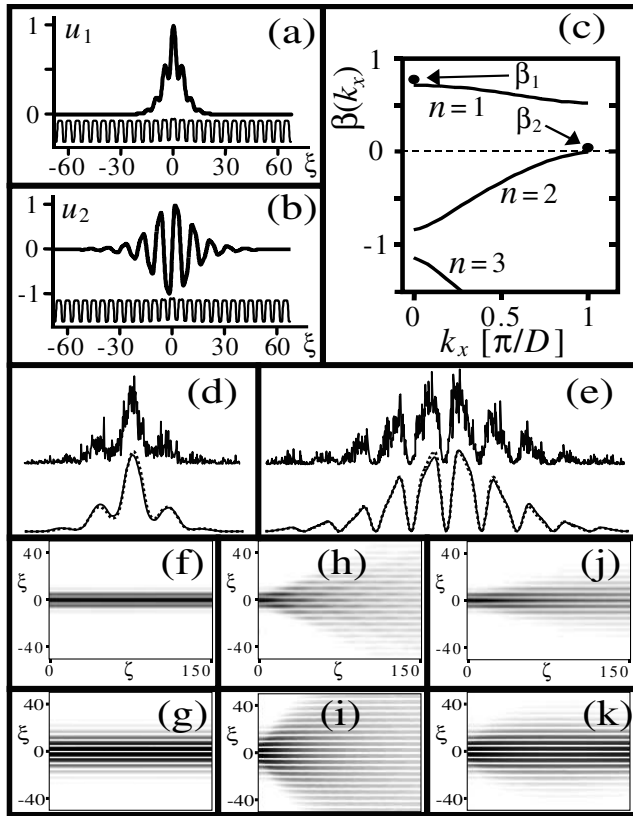


FIG. 2. Multiband vector lattice soliton in focusing waveguide array. (a),(b) Wave functions of the first u_1 and second u_2 components. (c) Dispersion relation of the first two bands of the linear array, with the propagation constants of the two soliton components marked by dots. First (d) and second (e) component intensities launched with white noise (top) and at the output (bottom) superimposed on the unperturbed profiles obtained through self-consistency (dotted line), showing that the output intensities of both components are almost indistinguishable from those of the ideal vector soliton. (f),(g) Self-trapped propagation of the components u_1 and u_2 of the vector soliton. (h),(i) Linear diffraction of u_1 and u_2 , respectively, when the nonlinearity is zero. (j) Nonstationary propagation of u_1 with the nonlinearity “on” and u_2 absent, and vice versa (k).

that the second component does not self-trap alone. The vector soliton forms only when both components are present [Figs. 2(f) and 2(g)].

Next, we study the relation between the two components of the vector self-trapped solutions. Figure 3(a) shows the propagation constants, $\beta_{1,2}$, vs the peak intensity of the second component, I_2 . The different curves correspond to peak intensities of the first component, I_1 (0, 0.2, ..., 1). The curve with $I_1 = 0$ corresponds to a scalar self-trapped solution, originating from the second band and residing in the first gap. The scalar soliton originating from the first band (and residing in the semi-infinite total internal reflection gap) is described by solutions with $I_2 = 0$. Notice that the scalar self-trapped solution arising from the first band induces a defect, which creates a bound state for the mode from

the second band even in the limit $I_1 \rightarrow 0$. The same situation occurs with the self-trap solution arising from the second band, which is able to localize a state from the first band even in the limit $I_2 \rightarrow 0$. In addition, since the second component resides in a gap, its peak intensity I_2 has a maximum value (1.18) occurring when $I_1 = 0$ and decreases as I_1 increases. No such upper limit exists for I_1 (because the gap in which it resides is semi-infinite). Figure 3(b) shows the widths, $\Delta x_{1,2} = \sqrt{\int_{-\infty}^{\infty} x^2 u_{1,2}^2(x) dx / \int_{-\infty}^{\infty} u_{1,2}^2(x) dx}$, of the components vs I_2 . The different curves correspond to values of I_1 (0, 0.2, 0.4, 0.6, 1). The width of the first component significantly depends on I_2 only for small I_1 . When I_1 is strong ($I_1 \sim 0.4$) the first component is already confined into a single channel; hence its width cannot change significantly. The increase in width of the second component for large I_2 results from the fact that its propagation constant approaches the first band. The minimum width of the second component is obtained when its propagation constant is deep in the gap ($\beta_2 \sim 0.31$). This minimum width (\sim two periods) is approximately independent of I_1 . Note that some of these vector self-trapped solutions are mildly unstable [26].

Next, we present an example of bright vector solitons in a defocusing nonlinearity, with $\sigma = -1$, $I_1 = 0.2$ and $I_2 = 0.3$. Here, u_1 [Fig. 4(a)] is a localized mode arising from the first band with $k_x^{(1)} = \pi/D$, while u_2 [Fig. 4(b)] is a localized mode arising from the second band with $k_x^{(2)} = 0$. Figure 4(c) shows $\beta(k_x)$ of the first three bands, with the propagation constants of the two components of the soliton marked by dots. In this case, the defect is negative. Figures 4(d) and 4(e) show the stationary propagation of the two components with initial noise. The linear diffraction of u_1 and u_2 with zero nonlinearity is shown in Figs. 4(f) and 4(g). When one of the components is absent while the nonlinearity is on, the remaining component does not exhibit stationary propagation

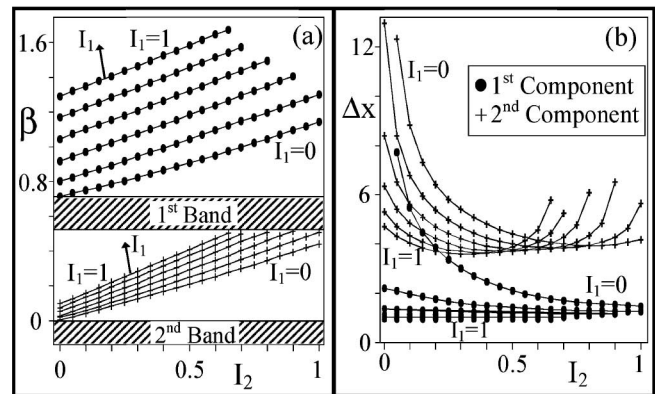


FIG. 3. Propagation constants (a) and widths (b) of the two components of a multiband vector self-trap solution in self-focusing media vs the peak intensity of the second component, I_2 . The different lines correspond to different peak intensities (between 0 and 1) of the first component, I_1 .

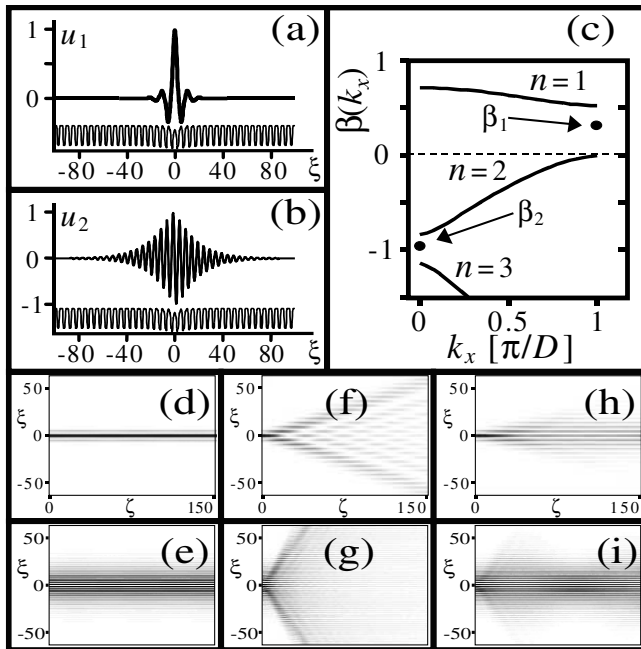


FIG. 4. Multiband lattice vector soliton in defocusing waveguide array. (a),(b) Wave functions of the first (u_1) and second (u_2) components. (c) Dispersion relation of the first two bands of the linear array, with the propagation constants of the two soliton components marked by dots. (d),(e) Self-trapped propagation of u_1 and u_2 of the vector soliton. (f),(g) Linear diffraction of u_1 and u_2 , respectively, when the nonlinearity is set to zero. (h) Nonstationary propagation of u_1 with the nonlinearity on and u_2 absent, and vice versa (i).

[Figs. 4(h) and 4(i)]. We carried out a systematic study of the relation between the two components of a multiband vector self-trap solution, similar to the study presented in Fig. 3. The findings resemble those discussed in the context of Fig. 3, with two exceptions: (i) since the induced defect is now negative, the propagation constants of both modes decrease as the modal intensities increase, and (ii) since both modes now reside in the gaps, both I_1 and I_2 have maximum allowed values (0.83 and 0.85, respectively).

Like coupled modes in excited quantum systems, these multiband vector lattice solitons (nonlinear modes in periodic potentials) should appear in a variety of experiments. The equivalence between soliton phenomena in nonlinear optics and in coherent quantum systems (particularly BEC) has been broadly discussed [27]. For example, results from excitation-relaxation experiments looking for nonlinear charge-density waves in atomic arrays [3] almost certainly contain contributions from these higher bands. In BEC, dark [28] and bright [29,30] matter-wave solitons have been observed. The recent demonstration of optically induced atomic lattices [31] makes the observation of matter-wave lattice solitons imminent. Equally important, multicomponent BECs have been observed in various settings [32]. Hence,

higher-band matter-wave solitons should be observed in the future. The theoretical foundation of such solitons, which incorporate radiation modes in their modal constituents, was the topic of this Letter [26].

This research was supported by the Ministry of Science, Israel, the MURI program on solitons, and by the German-Israeli DIP project.

-
- [1] A. S. Davydov, *J. Theor. Biol.* **38**, 559 (1973).
 - [2] D. N. Christodoulides and R. I. Joseph, *Opt. Lett.* **13**, 794–796 (1988).
 - [3] W. P. Su, J. R. Schieffer, and A. J. Heeger, *Phys. Rev. Lett.* **42**, 1698 (1979).
 - [4] A. Trombettoni and A. Smerzi, *Phys. Rev. Lett.* **86**, 2353 (2001).
 - [5] H. Eisenberg *et al.*, *Phys. Rev. Lett.* **81**, 3383 (1998).
 - [6] D. N. Christodoulides *et al.*, *Nature (London)* **424**, 817 (2003).
 - [7] A. A. Sukhorukov and Y. S. Kivshar, *Phys. Rev. Lett.* **87**, 083901 (2001); *J. Opt. Soc. Am. B* **19**, 772 (2002).
 - [8] Y. S. Kivshar, *Opt. Lett.* **18**, 1147 (1993).
 - [9] J. W. Fleischer *et al.*, *Phys. Rev. Lett.* **90**, 023902 (2003).
 - [10] S. Darmanyan *et al.*, *Phys. Rev. E* **57**, 3520 (1998).
 - [11] J. Meier *et al.*, “Discrete Vector Solitons in Kerr Nonlinear Waveguide Arrays,” *Phys. Rev. Lett.* (to be published).
 - [12] D. Mandelik *et al.*, *Phys. Rev. Lett.* **90**, 053902 (2003); **90**, 253902 (2003).
 - [13] N. K. Efremidis *et al.*, *Phys. Rev. E* **66**, 46602 (2002).
 - [14] F. Bloch, *Z. Phys.* **52**, 555 (1928).
 - [15] In a 1D system; in higher-dimensional systems the transport properties are considerably more complex.
 - [16] T. Iizuka and M. Wadati, *J. Phys. Soc. Jpn.* **66**, 2308–2313 (1997).
 - [17] G. I. Stegeman and M. Segev, *Science* **286**, 1518 (1999).
 - [18] A. W. Snyder, S. J. Hewlett, and D. J. Mitchell, *Phys. Rev. Lett.* **72**, 1012 (1994).
 - [19] V. Manakov, *Sov. Phys. JETP* **38**, 248 (1974).
 - [20] D. N. Christodoulides *et al.*, *Appl. Phys. Lett.* **68**, 1763 (1996).
 - [21] U. Kang *et al.*, *Phys. Rev. Lett.* **76**, 3699 (1996).
 - [22] Z. Chen *et al.*, *Opt. Lett.* **21**, 1436 (1996).
 - [23] D. N. Christodoulides and R. I. Joseph, *Opt. Lett.* **13**, 53 (1988); M. Haelterman, A. P. Sheppard, and A. W. Snyder, *Opt. Lett.* **18**, 1406 (1993).
 - [24] M. Mitchell *et al.*, *Phys. Rev. Lett.* **79**, 4990 (1997).
 - [25] M. Mitchell, M. Segev, and D. N. Christodoulides, *Phys. Rev. Lett.* **80**, 4657 (1998).
 - [26] Note related work A. A. Sukhorukov and Y. S. Kivshar, following Letter, *Phys. Rev. Lett.* **91**, 113902 (2003).
 - [27] P. Meystre, *Atom Optics* (Springer-Verlag, New York, 2001).
 - [28] S. Burger *et al.*, *Phys. Rev. Lett.* **83**, 5198 (1999).
 - [29] K. E. Strecker *et al.*, *Nature (London)* **417**, 150 (2002).
 - [30] L. Khaykovich *et al.*, *Science* **296**, 1290 (2002).
 - [31] M. Greiner *et al.*, *Nature (London)* **419**, 51 (2002).
 - [32] D. S. Hall *et al.*, *Phys. Rev. Lett.* **81**, 1539 (1998).